

ECG & HEART SOUNDS

FINAL REPORT

KEREN DRUKER - 208678847

LIOR BEN ISHAY - 313135261

1 Abstract

In this paper, we introduce an approach for the analysis and processing of electrocardiogram (ECG) signals and heart sounds, with the primary objective of diagnosing various cardiac conditions and assessing heart functionality. We provide a comprehensive overview of the physiological and pathological aspects of the cardiac cycle, emphasizing the significance of ECG signals and heart sounds in clinical practice. Additionally, we discuss the sources and types of noise that can impact these signals. The central research questions addressed in our study pertain to the effectiveness of the proposed method in detecting cardiac abnormalities and its potential implications for early disease detection. The rationale behind our research lies in the need to enhance existing diagnostic techniques, reduce healthcare costs, and improve global accessibility to cardiac care. To achieve these goals, we outline the materials and methods employed, including the BIOPAC system, the QRS detection algorithm, heart rate variability (HRV) calculations, and heart sound detection algorithms. Experimental data collected from participants in various states (e.g., sitting, standing, and during heavy breathing) are analysed and discussed. The results highlight the accuracy and reliability of the proposed method, emphasizing its potential clinical utility. In conclusion, our research contributes to the field of cardiac analysis by offering an effective approach for evaluating ECG signals and heart sounds. By leveraging this method, clinicians can enhance diagnostic precision, leading to improved patient outcomes and better management of cardiovascular diseases.

2 Introduction

Electrocardiogram, also known as ECG, is a non-invasive method to record the electrical activity of the heart that can be used to diagnose various heart conditions (e.g. heart failure, irregular heartbeat, heart murmur) and functionality. An ECG is performed by attaching electrodes to a patient's body, on different spots, usually chest, arms, and legs, and detect the voltage differences between those reference points. The configuration of two electrodes (one positive and one negative) relative to a third electrode (the ground) is called "Lead". The electrode positions for the different leads have been standardized and classified by numbers (Lead I, Lead II, etc.). The shape of the ECG signal is created due to the electrical conduction pathway in the heart and consists of P wave, QRS complex and T wave, periodically, as shown in figure 1. [1] Modern ECG machines record signals in frequency range of 0.05 – 150 Hz as a standard, and can vary based on filtering or measuring techniques. In order to get reliable results, special care should be taken regarding the sample rate. Therefore, we will use the Nyquist theorem, states that the sampling rate has to be greater than twice the highest frequency value in our signal (also called the Nyquist Frequency). Following this guideline, we can avoid phenomenon called Aliasing – a signal distortion occurs when the sampling rate is lower than Nyquist frequency as mentioned above, and might harm the reliability of the results. [2] Based on the information above, we can indicate that our sample rate should be larger than 300 Hz (twice the highest standard frequency).

The heart is muscular organ that pump blood through the body in two loops, the first one is the “Pulmonary circuit” which transports blood through the lungs, and “Systemic circuit” to oxygenate the blood in the tissues through the aorta (the largest blood vessel in human body). In order to provide blood into those circuits, the heart is separated into four chambers: two upper called atria and two lower called ventricles. To transport the blood along the body, those chambers contract and release in a process of depolarization and repolarization called the “cardiac cycle”. [3] This process involves the activity of four different valves, all of them function due to pressure differences between the heart chambers and vessels. The Tricuspid Valve, allowing the blood to flow between the right atrium and right ventricle, as well as preventing flow in the opposite direction. The Mitral Valve, allowing the blood to flow from the lungs to the left atrium, preventing flow from the left ventricle to the left atrium. Both of them are called the Atrioventricular valves. Two other valves are the Pulmonary Valve and the Aortic valve, allowing blood flow from the right ventricle to the lungs and from the left ventricle to the aorta, respectively. Both also prevent blood flowing backward. [4]

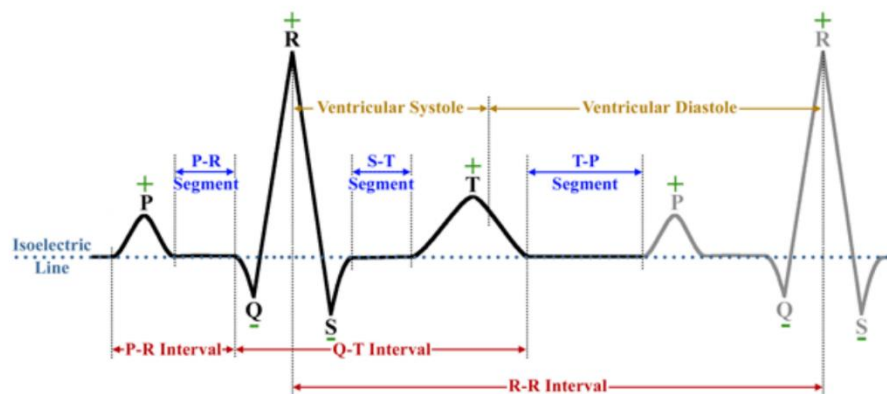


Fig 1. Normal ECG diagram with its components, figure 5.2 in [3] page 3.

The cardiac cycle occurs repeatedly and is triggered by an electrical sequence. The sequence starts with the sinoatrial node (SA node), also called the pacemaker, initiating the cardiac cycle by generating the electrical signal. In this stage, all the valves are closed. The pulse then spreads through the atrial muscle to the atrioventricular node (AV node), where it's delayed for 0.2 seconds. In this transition the atrial muscle contract, causing pressure difference between the chambers and therefore the opening of the tricuspid and mitral valves, then the blood flow to the ventricles – This is the first wave in the cardiac cycle, and it's marked with the letter P (figure 1). The content of P waves usually contains within 5-30 Hz frequencies. Then, the signal moves to the ventricles through the Purkinje system causing the ventricles to contract, thus pressure differences leading to the Atrioventricular valves closure and Pulmonary and Aortic valves open - This is the second wave in the cardiac cycle, representing the QRS wave (figure 1). The content of QRS waves mostly lays between 8-50 Hz. The last step is the depolarization of the ventricles, followed by closing the Pulmonary and Aortic valves (the Atrioventricular valves remain closed as described above), completing one period of the cardiac cycle, and representing the T wave (figure 1). The frequencies that characterize the T wave are mainly in the range of 0 to 10 Hz. [5] [2] [3] While ECG is the record of the electrical cycle of the cardiac cycle, the heart has a mechanical cycle in parallel, which is expressed by the heart sounds. In order to understand how does the mechanical cycle and the electrical cycle are related to each other, We will first elaborate on the heart sounds. There are 4 heart sounds marked as S1, S2, S3 and S4. Those sounds differ in their power, pitch, and length. To hear the heart sounds, a stethoscope is usually used and in general, only the first 2 sounds S1 & S2 will be heard. S1 is the first, longest and loudest heart sound and it reflects the tricuspid and mitral valves closure at the ventricular contraction, while the closure of the mitral valve is the more dominant one. It is characterized by low frequencies and

therefore low pitch. Since the loudness of the heart sound is related to the pressure difference and the contracted muscle size, Based on the explanation above, we can conclude that S1 sound is the loudest. Moreover, we can conclude that S1 corresponds to the QRS complex in the ECG diagram. S2 reflects the closing of the Pulmonary and Aortic valves at the end of the ventricular contraction and therefore corresponds to T wave in the ECG diagram. S2 has higher frequency than S1, and therefore a higher pitch, it is shorter and slightly softer than S1. S1 and S2 are commonly characterized with a “lub-dub” sound usually heard when using a stethoscope, where S1 is the “lub” and S2 is the “dub”. S3 and S4 are much harder to detect, with very low pitch and amplitude and shorter than S1 and S2. S3 reflects the ventricles filling with blood at the depolarization of the ventricles, occurring right after S2 and corresponding to the part right after the T wave. S4 reflects the turbulence of blood in the contraction of the atria to the ventricles, corresponding to area between the P wave and the QRS complex. [3][6]

When measuring ECG, there are few common types of noises, which are predominant in ECG signal: Electromyographic noise (EMG), also known as Muscle tremor, is caused by electrical activity of skeletal muscles, usually when contracting them or sudden body movement. This kind of noises are characterized with frequencies within the range of 0.01-100 Hz and mainly overlapping with frequencies of QRS complexes which makes them hard to detect. Another type of noise is Powerline Interference, caused by the electrical power system our device is working with, and also from nearby electrical devices. The interference will appear as a sinusoidal noise consisting of 50 or 60 Hz. It is narrowband and might lead to wrong analysis of the ECG signal and therefore some precautions are usually taken to minimize its effect, such as: add grounding point, avoid loops in the leads cables and shield them, keep away from electrical device and more. An additional common type of noise is called Baseline Wander (BW). This noise interferes with the recorded ECG signal and can cause changes in the shape of the signal, mainly by drifting the isoelectric line up and down. This phenomenon is caused mainly by respiration and some other physiological factors that affect the signal with low frequency changes ($\sim 0 - 0.7$ Hz). BW makes it difficult to diagnose cardiac diseases accurately and lead to errors in heart condition diagnosis. [7] [8] [9] [10]

In this following paper, we would like to accomplish the following goals: First we would like to record ECG signals on different states, and evaluate a heart rate (HR) calculation using QRS complex detection and noise reduction algorithms on the collected data. Second, We would like to measure the heart rate variability (HRV) which is the variation in time between adjacent heartbeats [11], as well as assessing the signal to noise ratio (SNR). Last, using a Detection algorithm of the 1st and 2nd heart sound, we would like to analyze the heart functionality in different states.

3 Materials and methods

Throughout the experiment we have used the BIOPAC system including 2 SS2L electrode lead set, 6 disposable vinyl electrodes (EL503), electrode gel and extract information using BIOPAC Students Lab System. The experiment was divided into 3 parts: Varied conditions ECG signal acquisition, Finding HRV and SNR Enhancement and Heart Sounds Examination. The initial setup and calibration process was done by connecting the participant to the BIOPAC system through the SS2L lead set, and EL503 electrodes. The electrodes were placed so we could measure leads I and III (as described in the Introduction). As the participant maintained a calm posture and breath through their nose, a 30 seconds ECG signal capture was performed, followed by 10 seconds signal capture while the participant is standing and breathing normally and additional 10 seconds capture standing and breathing deeply. The capture between the sitting state and standing state was suspended for a few seconds to prevent a sharp and sudden change of the signal capture. For the second part of the experiment, an initial setup and calibration process was performed once again, followed by a 1-minute

ECG signal capture while the participant maintained a calm posture and breath through their nose. The third part was conducted using a stethoscope, initiated by listening to the heart sounds of the participant and finding the optimal location to hear the first (S1) and second (S2) heart sounds. This was done while the participant is sitting and breath normally. A set of electrodes were placed to measure Lead II, then the participant was connected to the BIOPAC system using one set of SS2L lead set and a digital stethoscope. After calibrating the system, a 20 seconds capture of ECG signal of Lead II was conducted, then the capture was suspended, as the participant performed light physical activity of jumping in place for 60 seconds. Right after, the participant sat up and an additional 10 seconds ECG signal capture was made.

During the experiment execution, the participant is a male, 29 years old, 178 cm tall and weighed 68 kg.

Data Analysis

In this section we will present the methods, formulas and algorithms we have used to analyze and process our data. The reasons we chose those tools are explained explicitly in the discussion section. First, we used a band-pass filter to remove low-frequency noise, including baseline wander and motion artifacts, and remove high-frequency noises. Another important equation we have used throughout the experiment was the Einthoven law, also known as the Einthoven Triangle, and determine the relation between leads I, II and III, in the following relation:

$$\text{Lead I} + \text{Lead III} = \text{Lead II} \quad (1)$$

Einthoven law states that the electrical current in Lead I and III is equal to the electrical current in Lead II. [3] Moreover, we have used several algorithms in order to analysis our data. First, we have used a band-pass filter (BPF) to remove low-frequency noise, including baseline wander and motion artifacts, by setting a lower cutoff frequency around 0.5 Hz to 1 Hz. In addition, to Remove high-frequency noise, such as EMG noise or electronic interference, by setting an upper cutoff frequency around 50 Hz to 150 Hz. For most ECG applications by applying a band-pass filter with these cutoff frequencies, we retained the most important frequencies of the ECG signal, which are generally in the range of 0.5 Hz to 40 Hz, where the clinically relevant information (P wave, QRS complex, and T wave) is found.

The QRS Detection Algorithm chosen in this work is AF2, method devised by Fraden and Neuman [12]. This algorithm is based on amplitude and first derivative and work as follows - First, an amplitude threshold is set to be 0.4 the maximum value of the ECG signal:

$$\text{Amp threshold} = 0.4 \cdot \max[X(n)] \quad , 0 < n < 8191 \quad (2)$$

Where $X(n)$ is a vector of 8190 values, holding sample points of the ECG signal. Then a vector $Y0(n)$ is set to be the absolute value of $X(n)$ and represents the rectified signal. A low-level clipper is applied on the rectified signal $Y0(n)$ and stored in $Y1(n)$:

$$Y1(n) = \begin{cases} Y0(n), & Y0(n) \geq \text{Amp threshold} \\ \text{Amp threshold}, & \text{else} \end{cases} \quad , 0 < n < 8191 \quad (3)$$

The first derivative of the clipped signal is then calculated, using the formula:

$$Y2(n) = Y1(n + 1) - Y1(n - 1) \quad , 1 < n < 8191 \quad (4)$$

Finally, a QRS candidate is declared if $Y2(n)$ is greater than fixed constant threshold 0.7 for at least two consecutive points. Based on the information given above, one can conclude that $Y2(n)$ is in fact representation of R peaks in the ECG signal. As stated above, one of our goals is to be able to evaluate the Heart rate of the participant. We have done so, using the QRS complex detection, collected data over 109 cardiac cycles, and the following equations:

$$HR(i) = \frac{60}{R(i+1) + R(i)} [bpm] \quad (5)$$

Where R are the r peaks detected in QRS detection Algorithm. This method produces a HR vector for the ECG signal. To obtain the mean and standard deviation (STD), we utilized the following equations:

$$mean = \frac{\sum_{i=1}^n x_i}{n} \quad (6) \quad STD = \sqrt{\frac{1}{n} \sum_{i=1}^n (x_i - \bar{x})^2} \quad (7)$$

x_i represents the current HR (HR(i)) and n represents the number of heart rate samples. \bar{x} is 0. In order to determine the statistical difference of HR in different states, we will use a two-tailed t-test. Since there is a relation between 2 separate measurements, we chose to use the two-tailed version of t-test, using the following formula:

$$t = \frac{\bar{x} - \mu}{s/\sqrt{n}} \quad (8)$$

Where \bar{x} is the difference between the samples mean, μ is the null-hypothesized, s is the std of the difference between the samples, n is the number of samples differences. [14] As stated in this paper goals we would like to calculate the HRV and SNR of the sampled signal. Analyzing the HRV was done as follows: First, the signal was modified with noise reduction, baseline wonder handling and cutting the signal. Next, using the HR data vector and formulas (6) & (7), we calculated the average heart rate and its std, extracting the HRV. For the SNR, first we have calculated the mean voltage and std of the isoelectric part of one cardiac cycle. We did this in order to have an estimation for the noise's std of our signal record. Then, in order to find the SNR, we found the R peak value (max amplitude of the signal) and divided it with the noise's std:

$$SNR = \frac{R_{peak}}{STD_{noise}} \quad (9)$$

For detecting the first and second heart sounds we have used the following algorithm, based on work paper by Xinpei W. , Yuanyang L. and Churan S. [15] Initially, we reduced noises and filtered the relevant information based on the frequency range of s1 and s2. In order to do so we have used band pass filter. Following that the sampled signal was divided into small segments and an energy value which reflects the heart sound power was calculated for each segment. The energy calculation was done using the Shannon energy formula:

$$E_s = -\frac{1}{N} \sum_{i=1}^N x^2(i) \log x^2(i) \quad (10)$$

Where x is the signal sample normalized to the maximum absolute value of the signal, and N is the number of segments. Secondly, we have determined the maximum energy value of all the heart sounds segments with the following formula:

$$p_{ha}(t) = \frac{E_{hs}(t) - M(E_{hs}(t))}{S(E_{hs}(t))} \quad (11)$$

To improve the accuracy of detecting the position of s1 and s2, a threshold value called 'th' has been defined. For each segment, we compared its amplitude to the threshold value. If the amplitude was greater than the threshold, we set it to 1, otherwise, we set it to 0. This was done to achieve more precise detection for the positions of s1 and s2, those points are the potential s1 and s2 segments. Within the potential segments, the peak values were identified and classification of s1 and s2 was

conducted based on the following guideline: s1 follows short time interval and s2 follows longer time interval.

4 Results

4.1 Part 1 - The ECG signal

First, we plotted the raw data of the 3 leads. We measured lead I and lead III and via BioPac we calculated lead II. The calculation was done using equation (1), based on Einthoven law, described above.

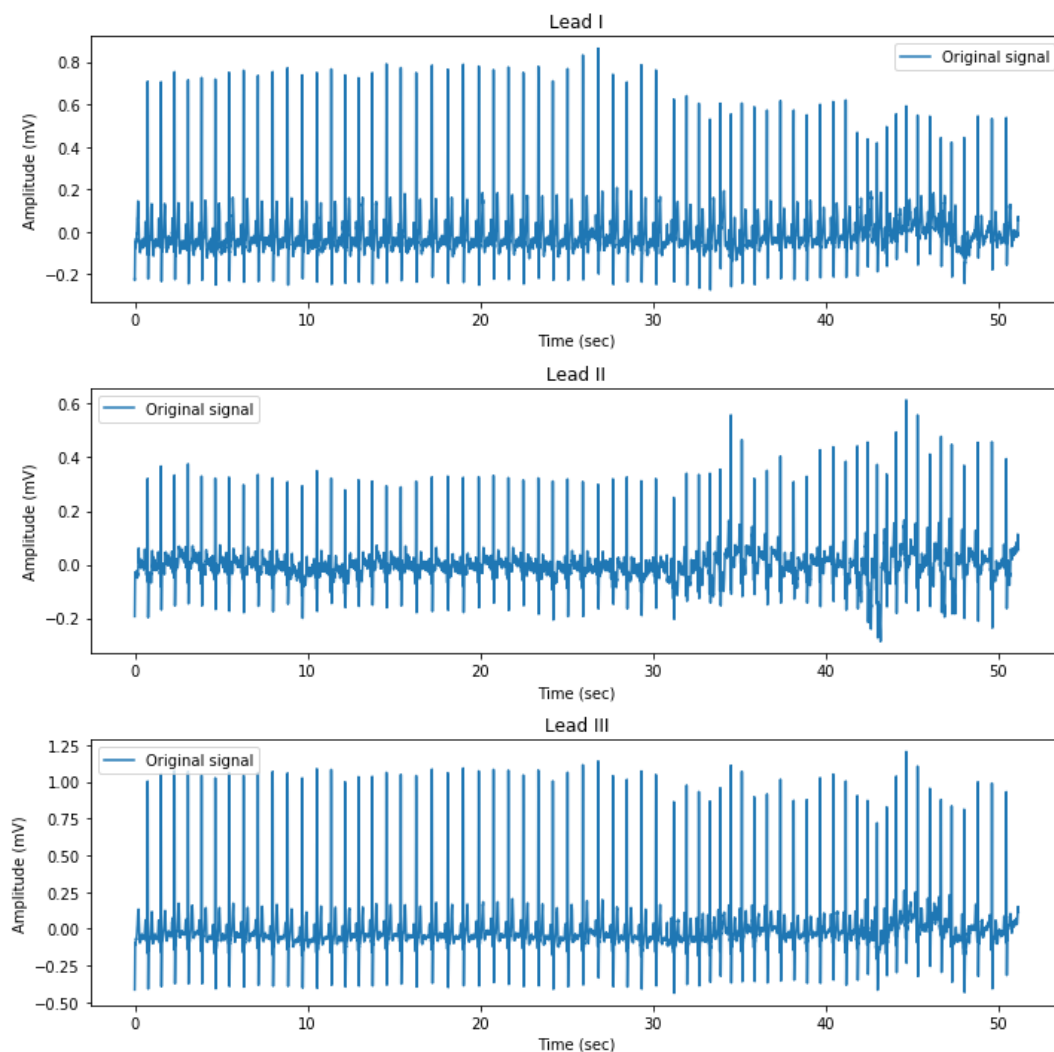


Figure 2. ECG original recordings

Using BPF, we were able to filter and reduce noise from the ECG sample shown in figure 2, received a filtered signal, that improves our ability to analyze the data correctly and thus get solid result and conclude reliable conclusions regarding our data. We applied those filters on Lead I, II and III and the filtered signals are shown in figure 3 below:

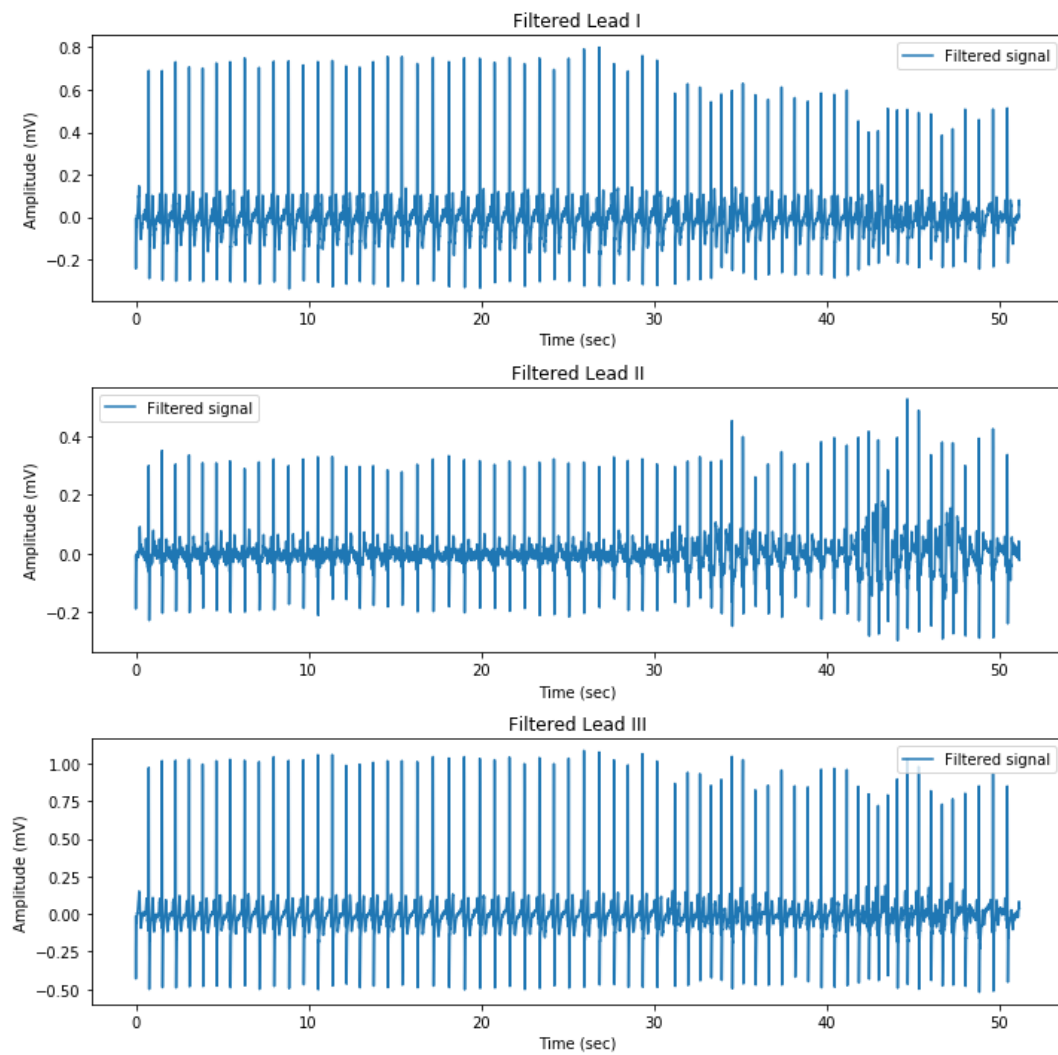


Figure 3. filtered ECG signal

The 3 leads ECG signals after using band pass filter:

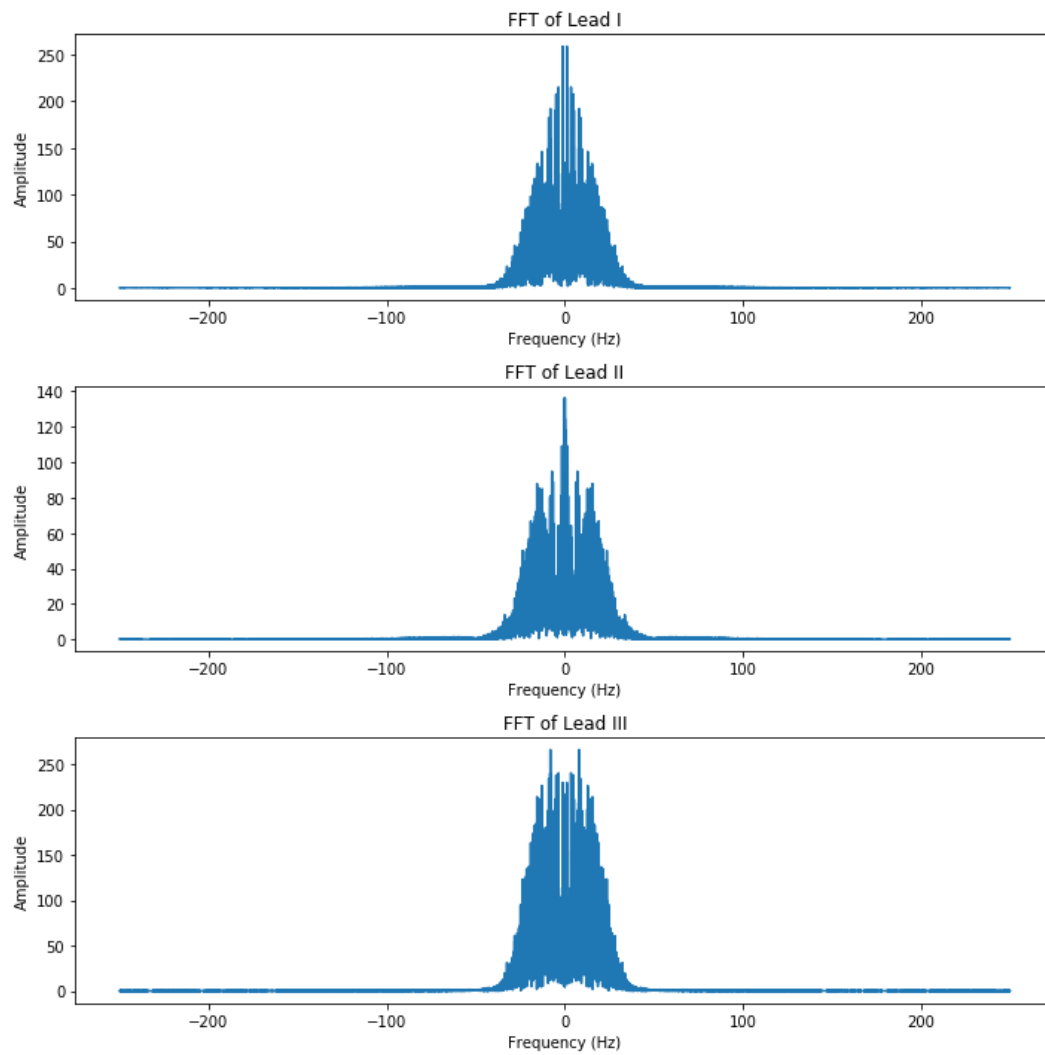


Figure 4. FFT of ECG signals recordings

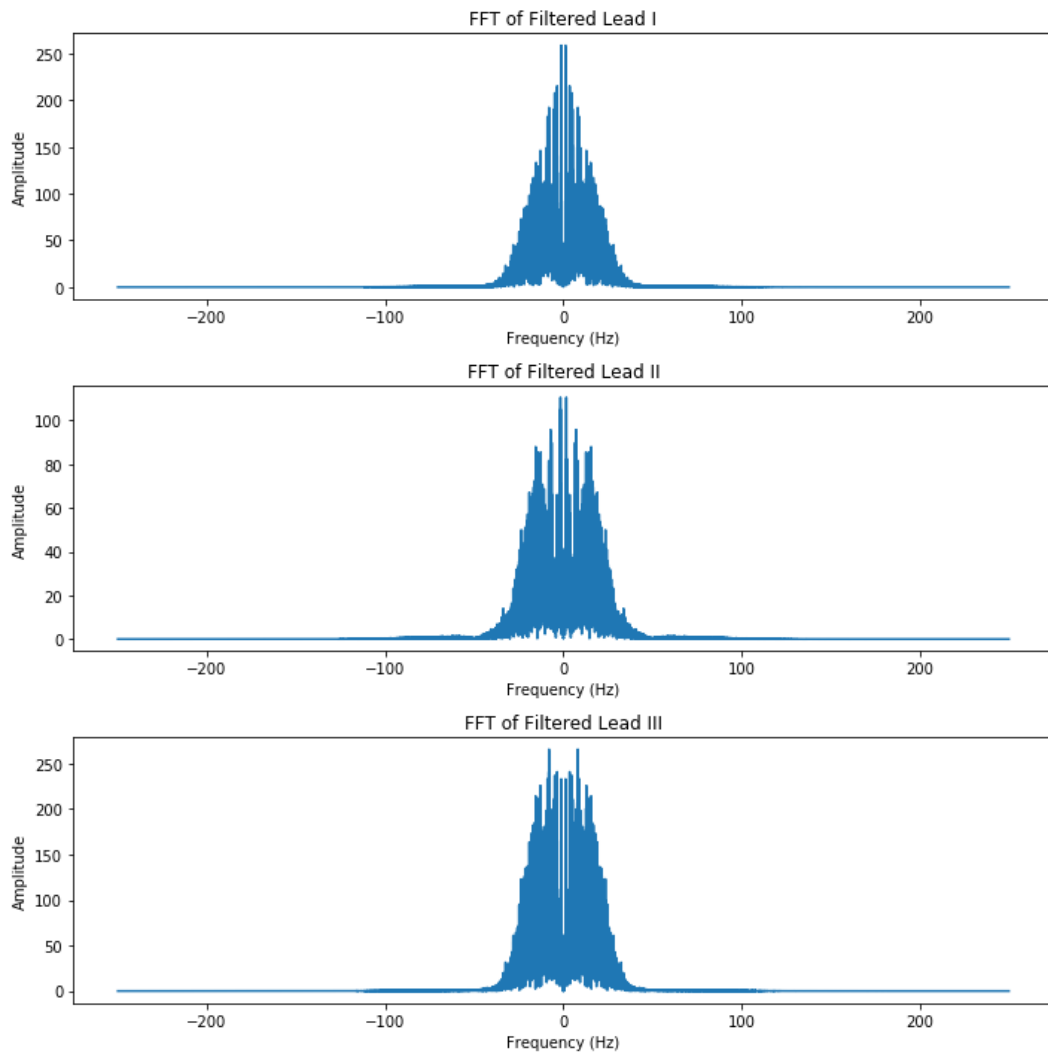


Figure 5. FFT of filtered ECG signals recordings

From this point we will continue with lead I. As stated above, we have used AF2 algorithm for R peaks detection:

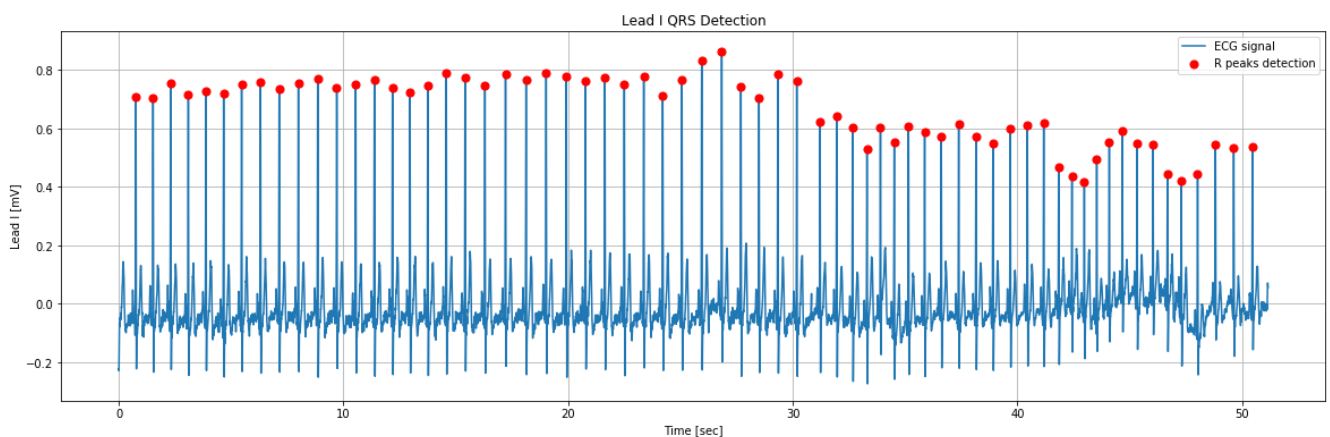


Figure 6. R-detection of the full lead I recorded.

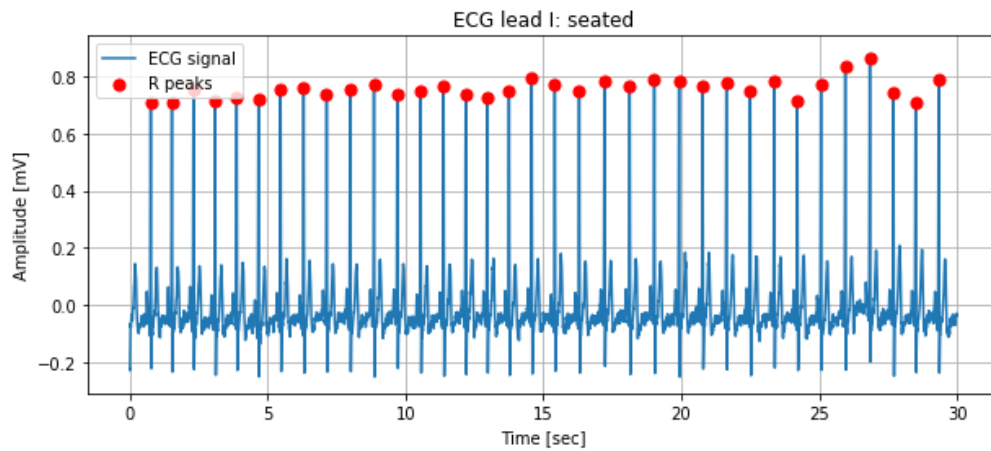


figure 7: R-detection of the sitting part of lead I recorded.

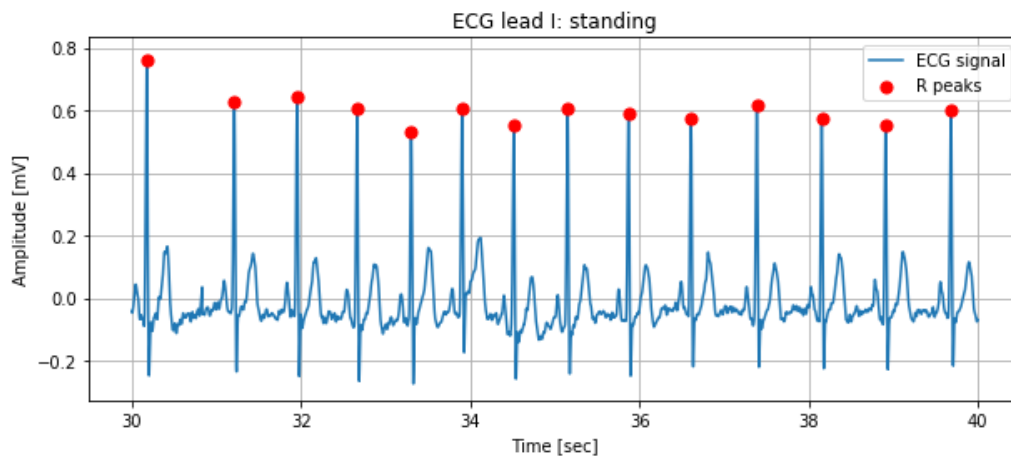


Figure 8. R-detection of the standing part of lead I recorded.

We have used the data of Lead I, separating the graphs based on the different states the participant maintained while taking the sample. Figures 7,8,9 represent seating, standing and heavily breathing states, respectively.

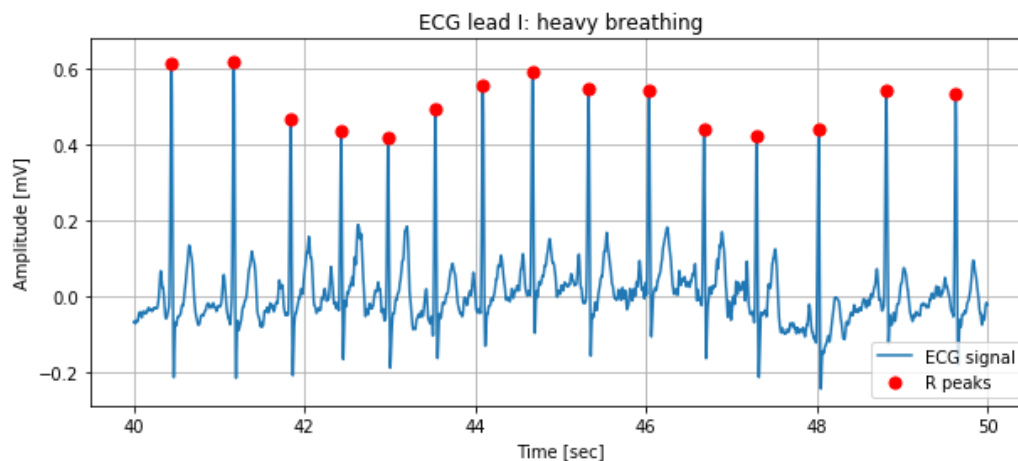


Figure 9. R-detection of the heavy breathing part of lead I recorded.

Using the measurements vector, and based on the theoretical background and formulas (6) & (7), we have calculated the mean and std of the HR in 3 different states: seating, standing and heavily breathing. The results are: *Seating*: 71.54 ± 3.44 , *Standing*: 83.6 ± 10.7 , *Heavy Breathing*: 92.91 ± 11.59 . Using the t-test formula (8) we can find the statistical difference between the HR of standing and heavy breathing: T-statistic: 2.08, P-value: 0.0478. There is a statistically significant difference between the HR of heavy breathing and standing.

4.2 Part 2 – HRV and SNR Statistics:

One of our main goals is to measure the heart rate variability (HRV), as well as assessing the signal to noise ratio (SNR). In order to do so, we recorded a 60 seconds ECG signal, in seating state, with calm breathing and minimum movements, as shown in figure 10 below:

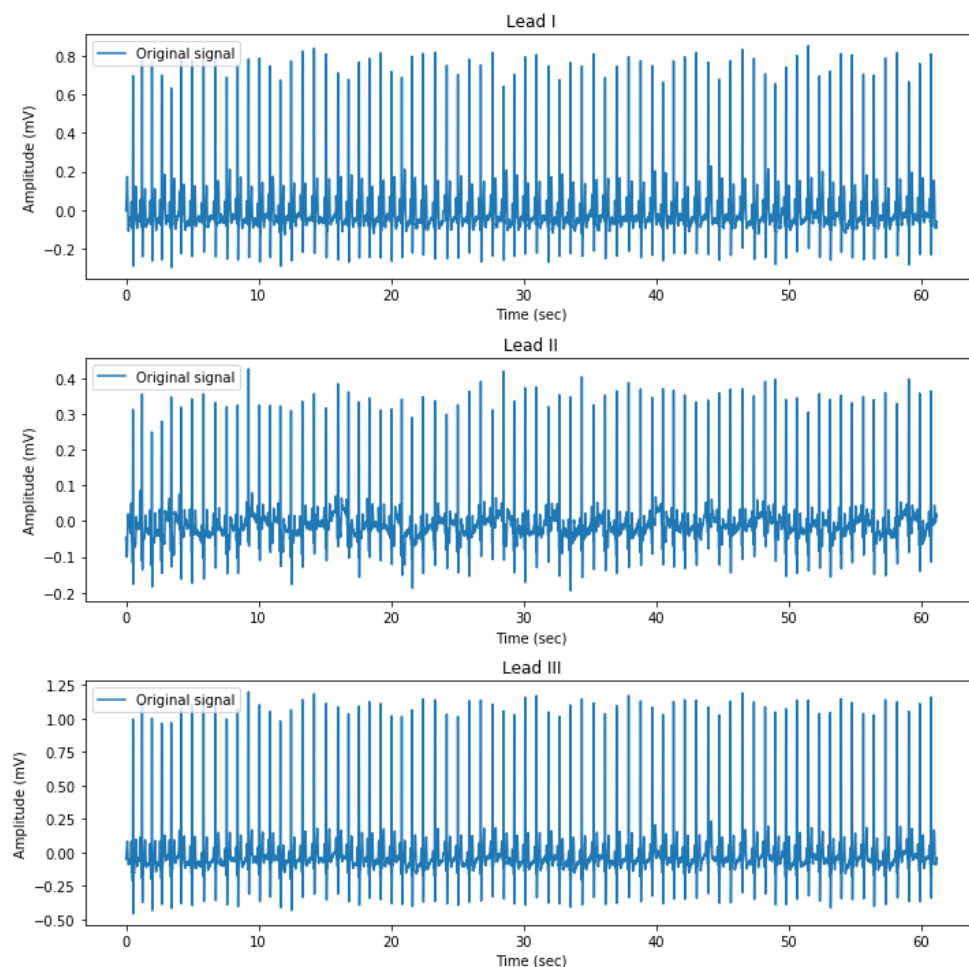


Figure 10. ECG signal record.

In this part, we will analyze only Lead I signal, as our data. We will elaborate about this choice in the discussion part. We have used BPF as we did before, in order to reduce noises and handle baseline wander. Using the data shown in figure 10, we were able to calculate the mean HR and its std, using the formulas (5) & (7) as described in the methods section. Thus, we got the following results:

$$\text{Mean HR: } 72.01 \text{ [BPM]} \quad , \quad \text{Standard Deviation of HR: } 4.27 \text{ [BPM]}$$

As can be seen from figure 11, 13 out of the 15 adjectives points are in the range of $mean\ HR \pm Std.$

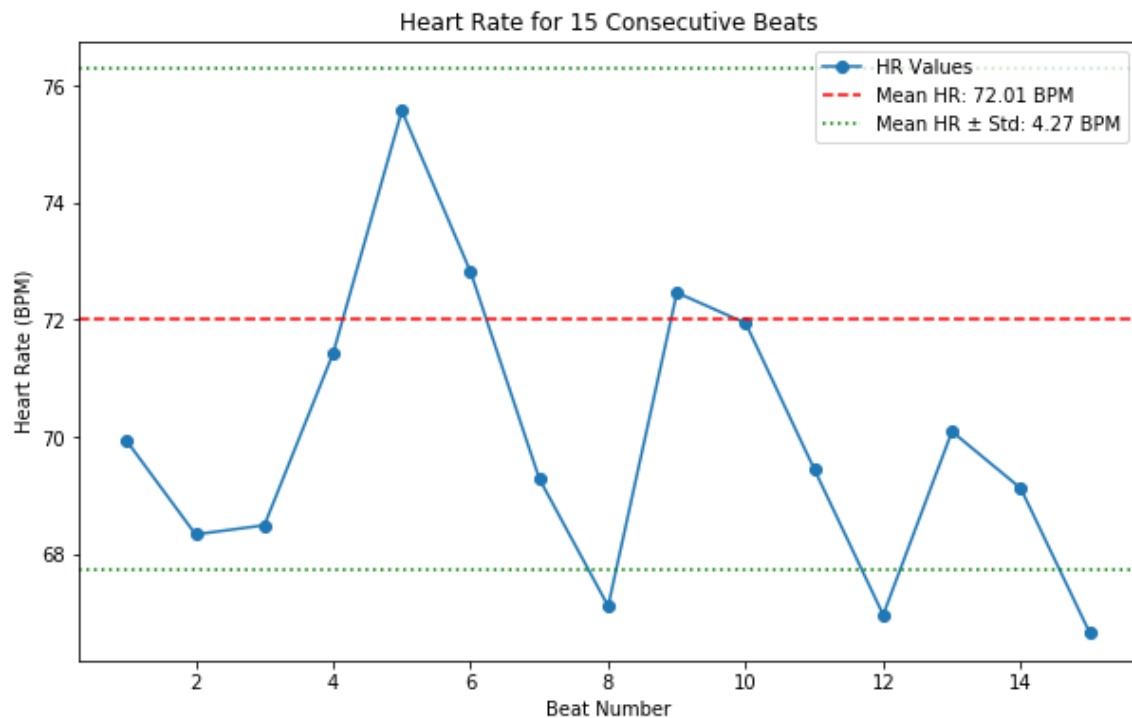


Figure 11. 15 heartbeats with the mean HR and std HR

Next, we have identified the R peaks in an ECG and selected a suitable window around them to encompass all the segments of a single cardiac cycle, including approximately 200 milliseconds before and 300 milliseconds after the R peak. Additionally, we have created an average signal of those sections (109 segments of a single cardiac cycle), resulting:

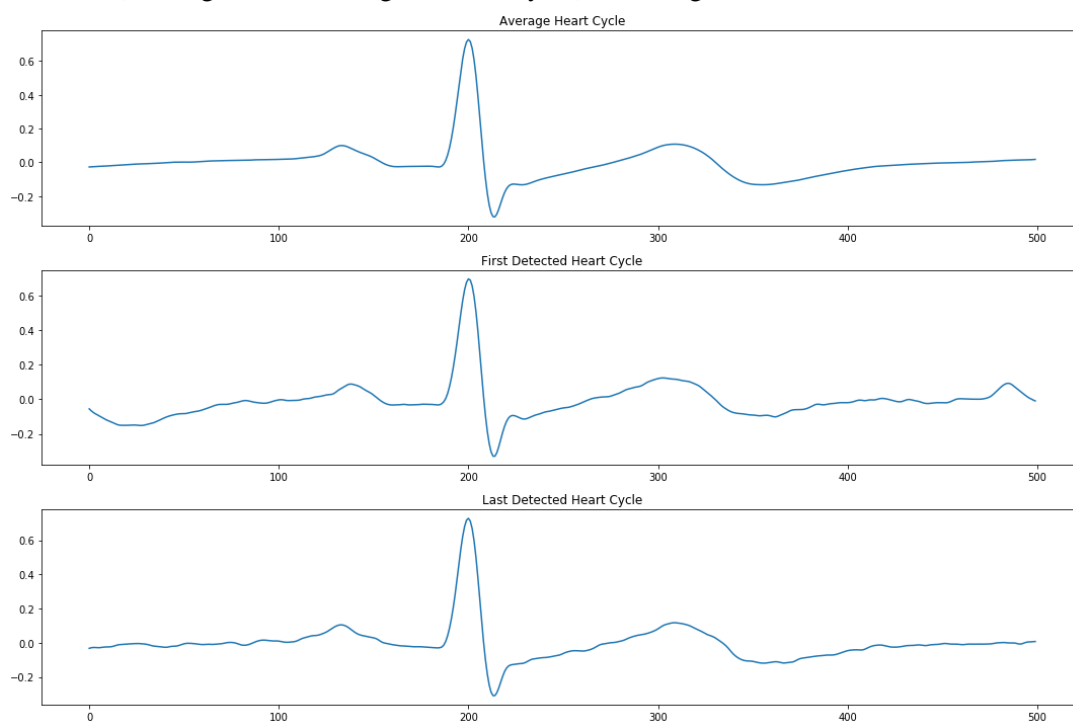


Figure 12. Average heart cycle, first heart cycle, last heart cycle

Using the Average Heart cycle signal, we have conducted some calculations on the isoelectric line. We chose the use the range of 50-100 first millisecond, reflecting the isoelectric line, and calculated the mean value of voltage and the std for the first, last and average heart cycles using the (6) & (7) formulas respectively:

First HB: -0.034 ± 0.023 , *Last HB:* -0.002 ± 0.009 , *Average HB:* -0.01 ± 0.005

From our results, we can see that the std of the average heart cycle signal was the lowest among the 3 signals (average, first, last), while the highest was for the first heart cycle. Evaluating the SNR values for the 3 different cases was done using the R peaks value for each case, as described on the methods section. Our results show that:

First HB SNR: 29.5 , *Last HB SNR:* 82.63 , *Average HB SNR:* 146.78

A plot for the SNR of the average heart rate signal is shown in figure 13:

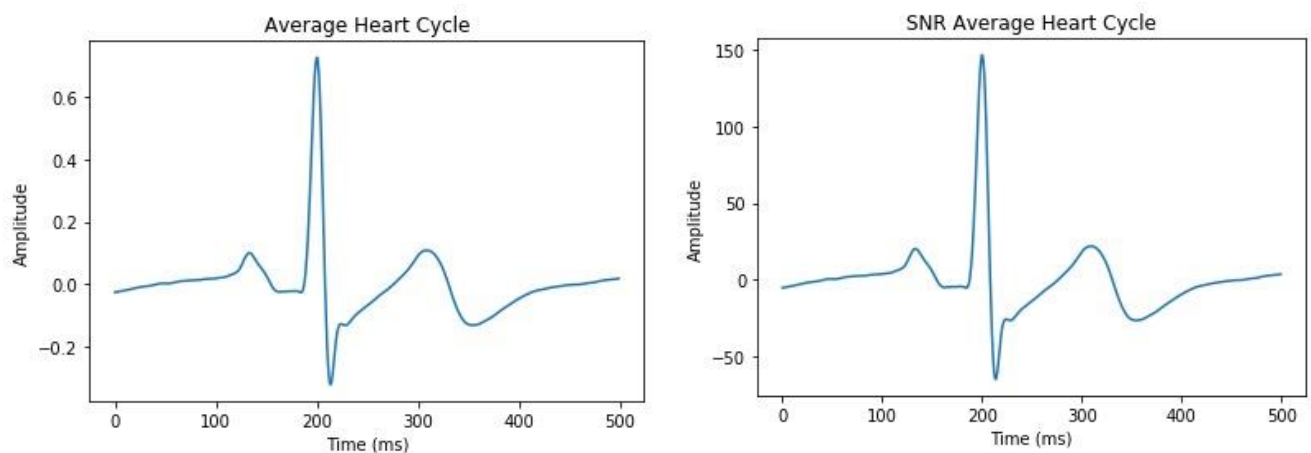


Figure 13. The average heart cycle signal (left) and the SNR of the heart cycle signal (right)

In figure 14, the improvement of SNR between the average HB and the first and last HB is shown:

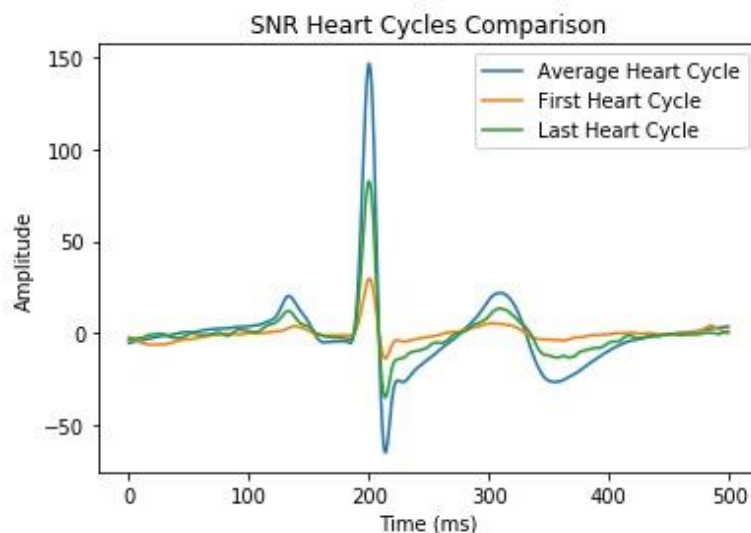


Figure 14. The improvement of the average heart cycle SNR relative to the first and last heart cycle SNR

4.3 Part 3 – Heart Sounds

Using the algorithm for detecting S1 & S2 heart sounds, we achieved the following results:

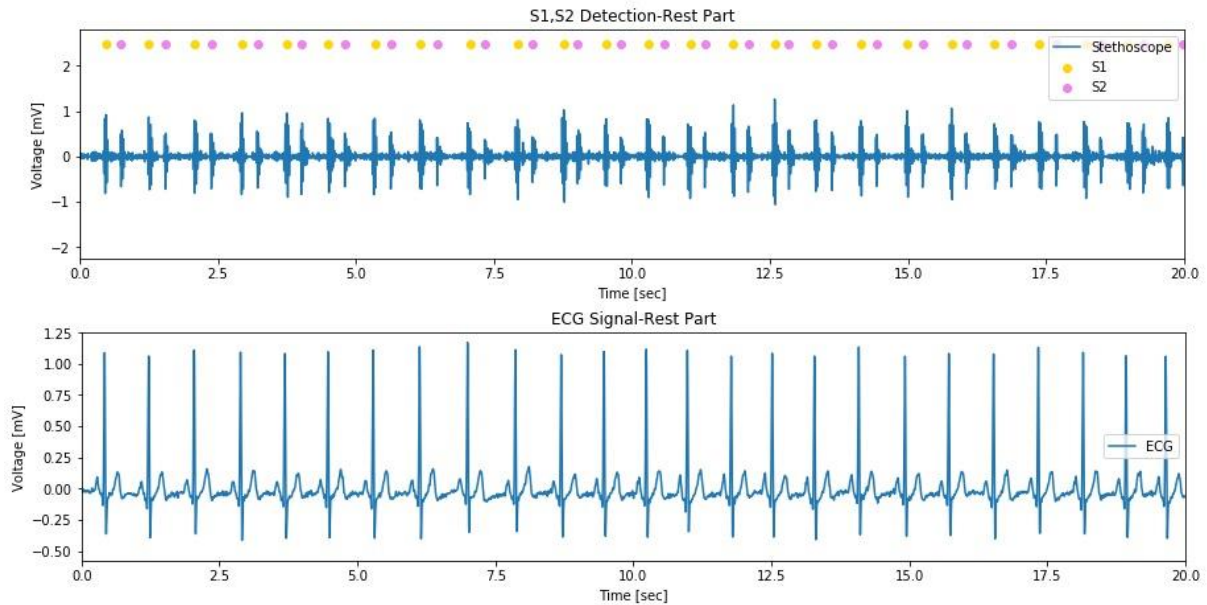


Figure 15. ECG signal and Heart sounds detection in Rest state

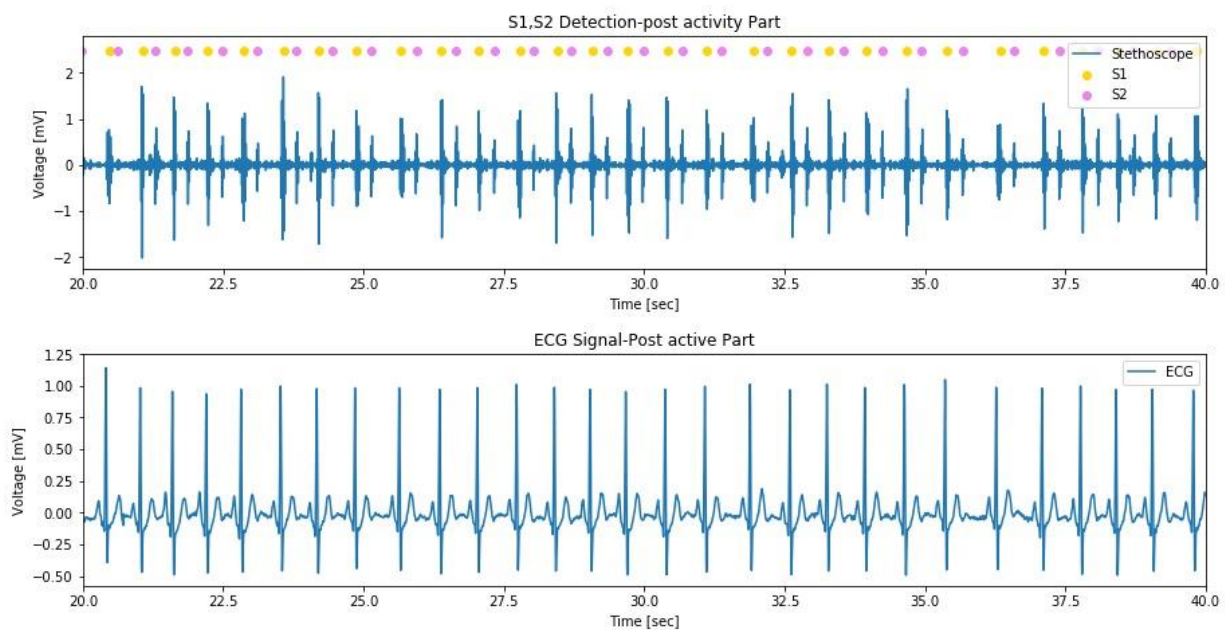


Figure 16. ECG signal and Heart sounds detection in Post-Activity state

As can be seen from the results shown in figure 15 and 16, the S1 & S2 heart sounds are marked on the upper graph (for each state), with the ECG signal on the lower graph for perspective.

Based on the results the S1 & S2 heart sounds detecting algorithm, we were able to measure the following values:

Measurement	At Rest (mean \pm std)	Post-exercise (mean \pm std)	Change in % between rest and post- exercise (based only on mean values)
BPM [# /min]	75.04 \pm 3.5	87.57 \pm 8.3	14.3%
ΔT R-wave to 1st sound [sec]	0.043 \pm 0.065	0.024 \pm 0.028	44.1%
ΔT R-wave to 2nd sound [sec]	0.157 \pm 0.18	0.153 \pm 0.168	2.5%
ΔT 1st to 2nd [sec]	0.284 \pm 0.019	0.253 \pm 0.111	10.91%
ΔT 2nd sound to next 1st sound [sec]	0.54 \pm 0.115	0.517 \pm 0.035	4.25%

Table 1. Measurements based on S1 and S2 detection results

We can see results matching the theory, as a further explanation and discussion will appear in the discussion section.

5 Discussion

Part 1 – ECG signal record

In this part of the experiment after doing calibration we recorded 50 seconds of ECG signal. The recording consisted of 30 seconds of the subject sitting still, 10 seconds of standing, and 10 more seconds of standing and heavy breathing. Figure 2 displays the ECG signal as recorded without any filter. The recording was in the frequency domain and had a sampling frequency of 500 Hz, which allowed us to convert it to the time domain. The record shows heartbeats patterns as we expected with P QRS and T waves as we detailed in the introduction part. It can be seen in the figure a baseline wander in all 3 leads particularly at the 10 last seconds of the record when the subject was heavy breathing.

As it seen in the results, the band pass filter removed the baseline wander and motion artifacts especially in leads I and III, as can be shown in Figure 3. We can see significant impact of filtering mainly at the end of the signal, and mainly noises caused by base wander. we chose to use a BPF. Since it is useful for signal extraction, filtering the unwanted high and low frequencies, thus filtering unwanted noises as described above. On the other hand, BPF is more complex (in terms of computational power) than other filters like IRR, so using it might require extra computational power.

The FFT (Fast Fourier Transform) of 3 leads of ECG signals provides insights into the frequency domain representation of the signals. This analysis is crucial for identifying abnormalities or specific characteristics related to heart conditions. DC Component- the distinct peak at zero frequency in all three plots indicates a strong DC component or low-frequency content. This could be due to baseline wander caused by factors like respiration or body movements. Frequency Components-the FFT reveals the different frequency components present in the ECG signals. These components can be associated with various physiological and pathological states of the heart. Comparison of Leads the

similar patterns but varying amplitudes in the FFT of Lead I, Lead II, and Lead III can provide comparative information about the electrical activity of the heart from different angles. As reviewed in the results section, filtering was a necessary part in order to conduct a reliable analysis of the ECG signal.

We have used AF2 algorithm for R peaks detection. We chose to use it for this purpose due to its significant advantages regarding QRS detection. Since the amplitude of the R peak is much higher than common noises (EMG, powerline, etc.), this algorithm successfully detects all the QRS complexes without any false-positive. Moreover, following the same reason above, it is very useful in filtering low frequency noises, which are common in ECG. Additionally, this algorithm is relatively simple and robust, and does not require complex calculations, thus very efficient in terms of execution time and computational power. Although it is useful and efficient, there are some disadvantages worth mentioning. Since it relies on filtering low amplitude, it has much lower effectiveness when filtering noises with similar or larger amplitude of the QRS complexes, and therefore can miss or detect false-positive QRS complexes in such cases. Additionally, Since the algorithm is based on an amplitude threshold, tuning the scaling constant of this threshold is necessary and might vary based on different noise type, make it difficult to get an adequate solution for all types of noises. [13] The fact that the algorithm relies on amplitude threshold and first derivative, resulting potential errors related to the resolution of those elements. In such cases QRS with low amplitude have the chance for false positive, as well as malfunction in case of some types of noises. In order to solve those issues, we can implement an adaptive threshold, adjusting throughout the process, based on previous QRS complexes and signal level. In the same way, we could suggest an adaptive derivative, make our system more sensitive to changes. Further inspiration for improvement can be taken from algorithms like "Digital Filter 1" [13], where a number of thresholds are used in order to detect the R peaks.

Part 2 – HRV and SNR

Remember, interpretation of FFT results should be done in conjunction with time-domain analysis and clinical information for accurate diagnosis.

In this part, we used only Lead I signal. We chose this signal from the 3 recorded signals, as it is relatively stable with the least noises impact. First, using figure 10 which represents a 60 seconds ECG signal of calm seating state, we have calculated the mean HR (72.01 bpm) and its std (4.27 bpm) as shown in the results section. Our results matched the theory as these measurements fall within the typical range for healthy adults at rest, indicating a well-balanced control of heart rate by the autonomic system. We assessed the SNR using spectral analysis on our ECG signal records. The noise signal was derived by analyzing the isoelectric line of average cardiac cycle from each segment as shown in figure 12. The isoelectric line was chosen to indicate the noise signal, as it represents a reference point for zero electrical activity of the heart. As anticipated, the std of the average HB was markedly lower than that of individual first HB or last HB, this is due to noise averaging over 109 segments of a single cardiac cycle. Our findings revealed a significant improvement of the SNR with the average heart cycle signal, 5 times larger relative to the first HB, and 1.78 times more than the last HB. This aligns with the visual ECG waveform morphology, which shows clarity and smoothness. Moreover, our results show larger amplitude of the SNR (Figure 14) for the average signal, which reflects the higher SNR value of it. Those findings confirm the theory, emphasizing that a high SNR improves the reliability of ECG analyses and cardiac diagnostics, indicative of robust signal quality and minimal noise interference. Conversely, a low SNR is an indication for inaccuracies and artifacts, caused by different noises, impairing the ECG assessments.

Following the conclusion shown above, one could suggest that implementing this method on additional segments will improve the result. As shown above, we do think a further improvement could be made if more segments were used, but since the standard deviation is relatively low, using more segments will have a small impact on the SNR value, which translate to only few percentages relative to the existing SNR, we have already achieved.

Part 3 – Heart Sounds

As shown in the Results section, figures (15) & (16), our algorithm successfully detected S1 and S2 heart sounds, based on the recorded signals, both in rest and post activity states. Using the results in table (1), it is noticeable that the heart rate increased (14.3%) between rest state and post activity state. Reflecting the increase in demand for oxygen as the theory suggests [3]. Moreover, we can see that the post-activity measurements related to the time intervals are decreased. This is aligned with the expected theory, claims that during exercise the ventricles depolarize more rapidly. Although the results we received follow the expected trend of higher HR and lower time intervals, the change in percentages is a bit low. We would expect to see more significant differences between the rest and post-activity states. One possible explanation is that the patient's exercise was insufficient in terms of effort, resulting in no substantial impact on their heart rate. Therefore, the results observed are insignificant as we expected. In further work, we would suggest to make sure that the exercise done by the participant will involve higher effort.

The heart sounds detection algorithm we have used, was described explicitly above, and was chosen based on its advantages: high ability to filter interference noises (heart murmurs and background noises) as well as 96 percent success in detecting S1 and S2 heart sounds. Some of its disadvantages are: low ability to detect heart murmurs, false-positive detection in case of abnormal heart sound patterns and highly interfering signal like crying or speech. [15] In practice, as the results shown, our algorithm successfully managed to detect all the S1 & S2 heart sounds appearances. We can attribute this to the fact that the filtered signal of the ECG had minimal noises and interference that helped to identify those heart sounds. A significant coherent problem with the algorithm described above is the fact that it effectively handles S1 & S2 sounds but not effective with S3 & S4. In future work, this algorithm could improve and include detection of S3 & S4 heart sounds, using new tools like Deep Learning neural networks, that will be trained on vast data set, and be able to include those sounds detection as well.

6 Conclusions

In this work we have proposed a method to analyze ECG sample in different states, extracting the HVR and SNR out of it, and detecting the 1st and 2nd heart sound using various algorithms. As shown in the results and elaborated in the discussion, using our method we were able to analyze with high precision the heart condition in different states and compare between those states. We have presented an effective algorithm to detect the 1st and 2nd heart sounds, and we discussed ways to improve the precision of our method, based on the result we got.

In the future, this method could be improved by focusing on the analysis part and include Deep Learning algorithms to optimize denoising, QRS complex detection and heart sound detection. Using this new technology, additional heart sound (3rd and 4th) could be detected, and it holds the potential for unprecedented use in cardiac analysis that can lead to early detection of Cardiovascular diseases, reduce healthcare cost, reach global accessibility and much more.

7 Bibliography

- [1] Junsang P., Junho A., Jinkook K., Sunghoon J., Yeongjoon G., Yoojin J., Kwanglo L. Il-young O., 2022. Study on the use of standard 12-lead ECG data for rhythm-type ECG classification problems, *Computer Methods and Programs in Biomedicine*; 214.
- [2] Tereshchenko, L. G., & Josephson, M. E., 2015. Frequency content and characteristics of ventricular conduction. *Journal of electrocardiology*; 48(6): 933–937. <https://doi.org/10.1016/j.jelectrocard.2015.08.034>
- [3] Pflanzner R, McMullen W, 2013. Physiology Lessons for use with the Biopac Student Lab, BIOPAC Systems; 5: 1-4.
- [4] Ho, I.S. 2011. Visualizing the cardiac cycle: a useful tool to promote student understanding. *Journal of microbiology & biology education*; 12 (1): 56–58. doi:10.1128/jmbe.v12i1.261.
- [5] Chan D., 2012. The cardiac cycle. *Anaesthesia and intensive care medicine*; 13 (8): 391–396.
- [6] Chizner MA. 2008. Cardiac auscultation: rediscovering the lost art. *Current Problems in Cardiology*; 33(7): 326-408. <https://doi.org/10.1016/j.cpcardiol.2008.03.003>
- [7] Mian Qaisar S. 2020. Baseline wander and power-line interference elimination of ECG signals using efficient signal-piloted filtering. *Healthcare technology letters* ; 7(4): 114–118. doi:10.1049/htl.2019.0116.
- [8] Singh B., Singh P. and Budhiraja S., 2015. "Various Approaches to Minimise Noises in ECG Signal: A Survey," *2015 Fifth International Conference on Advanced Computing & Communication Technologies*, pp. 131-137. doi: 10.1109/ACCT.2015.87.
- [9] Maggio A. C. V., Bonomini M. P., Leber E. L., Arini P. D., 2012. Quantification of Ventricular Repolarization Dispersion Using Digital Processing of the Surface ECG. "*Advances in Electrocardiograms - Methods and Analysis*" doi: 10.5772/23050.
- [10] Chatterjee S., Thakur R. S., Yadav R. N., Gupta L. and Raghuvanshi D. K., 2020. "Review of noise removal techniques in ECG signals", *IET Signal Process.*; 14(9): 569-590.
- [11] Mccratty R, Shaffer F. 2015. Heart Rate Variability: New Perspectives on Physiological Mechanisms, Assessment of Self-regulatory Capacity, and Health Risk. *Global Advances in Health and Medicine*; 4(1): 46-61. doi:10.7453/gahmj.2014.073
- [12] N. M. Fraden J, "QRS wave detection," vol. 18, no. 2, pp. 125-32, 1980.
- [13] Friesen, G. M., Jannett, T. C., Jadallah, M. A., Yates, S. L., Quint, S. R., & Nagle, H. T., "A comparison of the noise sensitivity of nine QRS detection algorithms," *IEEE transactions on bio-medical engineering*, vol. 37, no. 1, p. 85–98, 1990.
- [14] Kim T. K. 2015. T test as a parametric statistic. *Korean journal of anesthesiology*; 68(6), 540–546. <https://doi.org/10.4097/kjae.2015.68.6.540>
- [15] X. Wang, Y. Li, C. Sun and C. Liu. 2009 "Detection of the First and Second Heart Sound Using Heart Sound Energy," *2009 2nd International Conference on Biomedical Engineering and Informatics*; pp. 1-4, doi: 10.1109/BMEI.2009.5305640.